Using the current seasonal cycle to constrain snow albedo feedback in future climate change

Alex Hall and Xin Qu

Department of Atmospheric and Oceanic Sciences, University of California, Los Angeles, California, USA

Differences in simulations of climate feedbacks are sources of significant divergence in climate models' temperature response to anthropogenic forcing. One of these feedbacks, snow albedo feedback, is particularly critical for climate change prediction in heavily-populated northern hemisphere land masses. Here we show its strength in current models exhibits a factor-of-three spread. We also demonstrate that this spread may be dramatically reduced by exploiting the northern hemisphere springtime warming and simultaneous snow retreat in the current seasonal cycle as an analog for anthropogenic climate change: The large intermodel variations in snow albedo feedback's strength in climate change are nearly perfectly correlated with comparably large intermodel variations in its strength in the context of the seasonal cycle. Moreover, the feedback's strength in the real seasonal cycle can be measured and compared to simulated values. These mostly fall outside the range of the observed estimate, suggesting many models have an unrealistic snow albedo feedback in the seasonal cycle context. Because of the correlation between the feedback's simulated strength in the seasonal cycle and climate change, correcting these biases will lead directly to a reduction in the spread of snow albedo feedback simulations in climate change. Though this comparison to observations may put the models in an unduly harsh light because of uncertainties in the observed estimate that are difficult to quantify, our results map out a clear strategy for targeted observation of the seasonal cycle to reduce divergence in simulations of climate sensitivity.

1. Introduction

One reason convergence in simulations of climate feedbacks has eluded the climate modeling community [Bony et al., 2005; Stocker et al., 2001; Bony et al., 2004] is the difficulty in evaluating a feedback's simulated behavior against observations. The feedback is a feature of the future climate, and observations to evaluate it do not yet exist. We circumvent this by exploiting similarities between anthropogenic climate change and the present-day seasonal cycle. Both are examples of externally-forced climate variability, and it has been suggested that both are subject to the same climate feedbacks [Tsushima et al., 2005]. Support for this idea has been found recently in correlations between simulated seasonal cycle amplitudes and sensitivity to external forcing in the current generation of climate models [Knutti and Meehl, 2006].

In the case of snow albedo feedback (SAF), the seasonal cycle may be a particularly appropriate analog for climate change because the interactions of northern hemisphere (NH) continental temperature, snow cover, and broadband surface albedo (α_s) in the context of the seasonal variation of insolation are strikingly similar to the interactions of these variables in the context of anthropogenic forcing. As seen in fig 1, in the current climate northern hemisphere (NH) snow cover retreats rapidly from a maximum in late winter to a minimum in late summer in direct response to increasing sunshine and associated warmer temperatures [Robinson et al., 1993]. This in turn decreases α_s over NH continents, further increasing absorbed sunshine and enhancing surface warming. Similarly, in nearly all previous simulations of future climate [Cess et al., 1991; Randall et al., 1994; Cubasch et al., 2001; Manabe and Wetherald, 1980; Manabe and Stouffer, 1980; Robock, 1983; Ingram et al., 1989], as well as those of the current Fourth Assessment Report (AR4) of the Intergovernmental Panel on Climate Change (fig 2), snow cover retreats almost simultaneously with anthropogenic warming over NH land masses, reducing α_s in these areas, and increasing the overall warming through enhanced absorption of solar radiation.

The strength of SAF can be quantified, whether it occurs in the context of the current seasonal cycle or anthropogenic climate change. We set forth a method for doing this calculation, and use the results to examine the simulated relationship between the strength of NH springtime SAF in climate change and seasonal cycle contexts in 17 of the models used in the AR4 assessment. If the strength of SAF in the seasonal cycle in any particular model is correlated with its strength in climate change, then comparison of simulated SAF strength in the seasonal cycle to observations provides a meaningful constraint on simulated SAF strength in climate change. The seasonal cycle offers considerable advantages in model-observation comparison because it recurs every year. The current satellite record is approximately two decades long, so that already enough realizations of the seasonal cycle have been sampled to provide statistically-stable estimates of SAF strength in the seasonal cycle context, and the situation will only improve as the observed climate record lengthens. We focus here on the springtime component of NH SAF because both snow extent and insolation are large at this time of year. Hence SAF during springtime is particularly effective, contributing approximately half of the total NH SAF to simulated global climate change [Hall, 2004].

2. SAF components

The strength of SAF can be quantified by the variation in net incoming shortwave radiation (Q) with surface air temperature (T_s) due to changes in α_s [Cess and Potter, 1988]:

$$(\frac{\partial Q}{\partial T_s})_{SAF} = -I_t \cdot \frac{\partial \alpha_p}{\partial \alpha_s} \cdot \frac{\Delta \alpha_s}{\Delta T_s} \quad (1)$$

where the subscript SAF is used to emphasize that the partial derivative refers only to changes in Q with T_s that occur due to changes in α_s, rather than changes in cloudiness or

0094-8276/05/$5.00

other factors that could affect solar radiation. The constant I_t is the incoming solar radiation at the top of atmosphere (TOA), and α_p is the planetary albedo. Eq. (1) allows SAF to be decomposed as the product of two terms. The first ($\partial\alpha_p/\partial\alpha_s$) represents the atmosphere's attenuation effect on anomalies in α_s, determined by the time-mean distribution of atmospheric absorbers of solar radiation, including clouds. The other ($\Delta\alpha_s/\Delta T_s$) is the change in α_s induced by a unit change in T_s, determined by surface processes.

Recently a highly accurate technique was developed to calculate $\partial\alpha_p/\partial\alpha_s$ given standard model output [Qu and Hall, 2005]. We use it to calculate springtime $\partial\alpha_p/\partial\alpha_s$ values in NH land areas for the AR4 transient climate change experiments (fig 3a). The intermodel variation in this quantity is small, with most models agreeing to within 10% that a given α_s anomaly results in an α_p anomaly one-half as large. This agreement occurs because the main factor controlling $\partial\alpha_p/\partial\alpha_s$ is the cloudless component of the atmosphere, where the various radiative transfer schemes used by the simulations converge in their handling of the atmosphere's interaction with upwelling solar photons [Qu and Hall, 2005]. Thus differences in cloud fields do not introduce significant differences in estimates of $\partial\alpha_p/\partial\alpha_s$. It is straightforward to calculate the second component of SAF ($\Delta\alpha_s/\Delta T_s$) in the climate change context based on springtime values of α_s and T_s averaged over NH land areas from the beginning and end of the AR4 transient climate change experiments (fig 3b). While there is general agreement in simulated estimates of $\partial\alpha_p/\partial\alpha_s$, there is a three-fold divergence in $\Delta\alpha_s/\Delta T_s$, with no clear preference for a central value. This wide divergence is probably due to differences in snow albedo parameterizations.

3. Seasonal cycle and climate change relationship

Because the $\Delta\alpha_s/\Delta T_s$ component is most responsible for the intermodel spread in simulations of SAF, we focus on this component in our assessment of SAF in seasonal cycle and climate change contexts. It is possible to calculate values of $\Delta\alpha_s/\Delta T_s$ in the seasonal cycle context by taking climatological changes in NH continental α_s from one month to another and dividing them by climatological changes in T_s between the same two months. Consistent with our springtime focus, we did this for April and May based on the 20th century portion the AR4 transient climate change experiments. This is a time of year when NH continental α_s decreases rapidly, while T_s increases quickly (fig 1). Fig 4 shows a scatterplot of these values against the transient climate change values of $\Delta\alpha_s/\Delta T_s$ of fig 3b. Intermodel variations in $\Delta\alpha_s/\Delta T_s$ in the seasonal cycle context are highly correlated with $\Delta\alpha_s/\Delta T_s$ in the climate change context, so that models exhibiting a strong SAF in the seasonal cycle context also exhibit a strong SAF in anthropogenic climate change. Moreover, the slope of the best-fit regression line is nearly one, so values of $\Delta\alpha_s/\Delta T_s$ based on the present-day seasonal cycle are also excellent predictors of the absolute magnitude of $\Delta\alpha_s/\Delta T_s$ in the climate change context. Apparently the thermodynamic response time of the snow pack is fast enough that the snow retreat and α_s reduction associated with the springtime increase in solar radiation and temperatures mimicks very closely the analogous process occurring in response to anthropogenic forcing and century-scale warming in every simulation.

To calculate an observed estimate of $\Delta\alpha_s/\Delta T_s$ in the seasonal cycle context, we took April and May α_s values from the satellite-based International Satellite Cloud Climatology Project (ISCCP) dataset (i.e. values from fig 1c). Nearly 20 years in length, this is the only observed time series long enough to provide a statistically stable estimate of climatological α_s. April and May climatological T_s (fig 1a) is easily extracted from reanalysis data. We also calculated an estimate of the statistical error arising from the time series' limited length, giving a 95% confidence range for the observed value. Three models are very close to the observed range, while eleven models have a significantly weaker SAF than observed. Three simulations appear to have an unrealistically strong SAF, though no model's SAF is stronger than the observed range by more than about 20%.

Caution must be exercised in this comparison, because there may be sources of error other than statistical uncertainty in the observed estimate of $\Delta\alpha_s/\Delta T_s$. Unfortunately these are nearly impossible to quantify, and must be evaluated qualitatively: Measurements of T_s are an unlikely source of systematic or random measurement error. T_s over the NH land masses is well-sampled in space and time and the measurements are accurate, so we expect the reanalysis product to provide highly reliable estimates of climatological T_s. Observations of α_s present a more likely error source. ISCCP α_s values are based on satellite measurements at a single visible channel, and a dependence of surface albedo on wavelength is assumed to convert these observations to a broadband value. This functional dependence is in turn derived from measurements of the Earth Radiation Budget Experiment, when shortwave radiative fluxes were measured simultaneously with ISCCP at seven visible and near infrared channels for the 1984-1989 period [Zhang et al., 2004]. This approach, though reasonable as reflectances measured at the ISCCP channel are highly correlated with reflectances at other wavelengths where solar energy is concentrated, may introduce errors. Because of these errors the actual range of uncertainty in observed values of $\Delta\alpha_s/\Delta T_s$ may be somewhat larger than the range shown in fig 4; however, it seems improbable that the range would broaden enough to include all the models. For example, for the models in the low end of the range of fig 4 to be considered realistic, ISCCP's climatological seasonal reduction in α_s from April to May seen in fig 1c would have to be too large by a factor of two.

4. Concluding Remarks

The difficulty in quantifying all errors in the estimate of climatological $\Delta\alpha_s/\Delta T_s$ points to a clear strategy for targeted observation of the climate system. A systematic campaign to establish the seasonal climatology of α_s with a high degree of precision and accuracy, either through improved utilization of existing measurements or new satellite instruments, will lead directly to identification of biases in simulations of SAF in the context of the seasonal cycle. And the high correlation between simulated SAF parameters in seasonal cycle and climate change contexts implies the models will converge in their simulations of SAF in climate change if these biases are addressed. This would reduce the divergence in simulations of future climate, particularly in large portions of the heavily-populated northern hemisphere land masses, where SAF may account for nearly half the simulated warming in response to increasing greenhouse gases [Hall, 2004].

Because the seasonal cycle is a case of externally-forced climate variability recurring on a much shorter time scale than that of anthropogenic climate change, observations of it accumulate relatively quickly, providing statistically stable estimates of relevant quantities. Therefore exploiting similarities between the seasonal cycle and anthropogenic climate change is a promising strategy for constraining other

Figure 1. Composite seasonal cycles of monthly-mean T_s (A), snow extent (B), α_s (C) for NH continents poleward of 30°N. The composite seasonal cycle of T_s is based on data obtained from the ERA40 reanalysis for the 1958-2001 period (http://data.ecmwf.int/data/d/era40_mnth). The composite seasonal cycle of snow extent is based on data obtained from Rutgers University Global Snow Lab (http://climate.rutgers.edu/snowcover) and were derived from NOAA weekly snow cover maps covering the 1972-2004 period. The composite seasonal cycle of α_s is based on the 1984-2000 ISCCP data set.

Figure 2. Time series of springtime-mean (MAM) T_s (A), snow extent (B), and α_s (C) averaged over the NH poleward of 30°N for the 20th, 21st and 22nd centuries as simulated by the GFDL CM2.0 scenario run. Time series of these quantities for the other 16 models shown in table 1 are very similar.

important radiative feedbacks affecting the extratropics, where seasonality is most pronounced. For example, sea ice albedo feedback is also a significant source of divergence in simulations of climate sensitivity to anthropogenic forcing, particularly in high latitudes [Holland and Bitz, 2003]. Like NH snow, sea ice in both hemispheres undergoes a large variation in response to the seasonal cycle of extratropical temperatures. If sea ice albedo feedback could be also constrained with the current seasonal cycle, this would substantially reduce divergence in simulations of extratropical climate change.

Acknowledgments. Alex Hall and Xin Qu are supported by U.S. National Science Foundation Grant ATM-0135136. Any opinions, findings, conclusions, or recommendations expressed in this material are those of the authors and do not necessarily reflect the views of the U.S. National Science Foundaion. We acknowledge the international modeling groups for providing their data for analysis, the Program for Climate Model Diagnosis and Intercomparison (PCMDI) for collecting and archiving the model data, the JSC/CLIVAR Working Group on Coupled Modelling (WGCM) and their Coupled Model Intercomparison Project (CMIP) and Climate Simulation Panel for organizing the model data analysis activity, and the IPCC WG1 TSU for technical support. The IPCC Data Archive at Lawrence Livermore National Laboratory is supported by the Office of Science, U.S. Department of Energy.

References

Bony, S. and coauthers, 2004: On dynamic and thermodynamic components of cloud changes. *Climate Dyn.*, **22**, 71–86.

Bony, S. and coauthers, submitted: How well do we understand climate change feedback processes? *J. Climate*.

Cess, R. D. and coauthors, 1991: Interpretation of snow-climate feedback as produced by 17 general circulation models. *Science*, **253**, 888–892.

Cess, R. D. and G. L. Potter, 1988: A methodology for understanding and intercomparing atmospheric climate feedback processes in general circulation models. *J. Geophys. Res.*, **93**(D7), 8305–8314.

Cubasch, U. and coauthors, 2001: Projections of future climate change. *Climate Change 2001:The Scientific Basis.* J. W. Kim and J. Stone, Eds., Cambridge University Press, 525-582.

Hall, A., 2004: The role of surface albedo feedback in climate. *J. Climate*, **17**, 1550–1568.

Holland, M. M. and C. M. Bitz, 2003: Polar amplification of climate change in coupled models. *Climate Dyn.*, **21**, 221–232.

Ingram, W. J., C. A. Wilson and J. F. B. Mitchell, 1989: Modeling climate change: an assessment of sea ice and surface albedo feedbacks. *J. Geophys. Res.*, **94**(D6), 8609–8622.

Knutti, R. and G. Meehl, submitted: Constraining climate sensitivity from the seasonal cycle in surface temperature. *J. Climate*.

Manabe, S. and R. J. Stouffer, 1980: Sensitivity of a global climate model to an increase of CO_2 concentration in the atmosphere. *J. Geophys. Res.*, **85**(C10), 5529–5554.

Manabe, S. and R. T. Wetherald, 1980: On the distribution of climate change resulting from an increase in CO_2 content of the atmosphere. *J. Climate*, **37**(1), 99–118.

Neter, J. and coauthors, 1996: Inferences in regression analysis. *Applied Linear Statistical Models. 4th Edition,* WCB/McGraw-Hill, 44-94.

Qu, X. and A. Hall, 2005: Assessing snow albedo feedback in simulated climate change. Accepted to *J. Climate*.

Randall, D. A. and coauthors, 1994: Analysis of snow feedbacks in 14 general circulation models. *J. Geophys. Res.*, **99**(D10), 20757–20772.

Robinson, D. A., K. F. Dewey and R. R. Heim, Jr., 1993: Global snow cover monitoring: An update. *Bull. Amer. Meteor. Soc.*, **74**(9), 1689–1696.

Robock, A., 1983: Ice and snow feedbacks and the latitudinal and seasonal distribution of climate sensitivity. *J. Atmos. Sci.*, **40**, 986–997.

Stocker, T. F. and coauthors, 2001: Physical climate processes and feedbacks. *Climate Change 2001:The Scientific Basis.* S. Manabe and P. Mason, Eds., Cambridge University Press, 417-470.

Tsushima, Y., A. Abe-Ouchi and S. Manabe, 2005: Radiative damping of annual variation in global mean temperature: Comparison between the observed and simulated feedback. *Climate Dyn.*, **24**(6), 591–597.

Zhang, Y.-C., W. B. Rossow, A. A. Lacis, V. Oinas and M. M. Mishchenko, 2004: Calculation of radiative fluxes from the surface to top of atmosphere based on ISCCP and other global datasets: Refinements of the radiative transfer model and the input data. *J. Geophys. Res.*, **109**(D19105), 1–27.

A. Hall, Department of Atmospheric and Oceanic Sciences, University of California, Los Angeles, PO BOX 951565, CA 90095-1565. (alexhall@atmos.ucla.edu)

Figure 3. A. The dependence of April α_p on α_s in NH land masses poleward of 30°N as seen in transient climate change experiments of the AR4 assessment for the 20th century, showing how large a typical α_p anomaly is for a 1% α_s anomaly in areas likely to be affected by SAF. The methodology [Qu and Hall, 2005] for this calculation requires α_s, cloud cover and cloud optical thickness data as well as TOA clear-sky and all-sky solar fluxes. These data were only available for 13 of the 17 simulations. We carried out the same calculation for other time periods of the experiments (not shown), and found that these values exhibit very little dependence on the time period chosen, so that simulated changes in cloudiness in response to anthropogenic forcing do not significantly affect the values shown here. It is also possible to use this method to calculate $\partial\alpha_p/\partial\alpha_s$ from data given by the satellite-based International Satellite Cloud Climatology Project (ISCCP), covering the 1984-200 period. This observed value is shown with a solid line, and is in general agreement with the simulated values. B. The externally-forced change in April α_s (%) averaged over NH land masses poleward of 30°N in transient climate change experiments of the AR4 assessment, divided by the change in April T_s in these experiments averaged over the same region. The change in α_s (or T_s) is defined as the difference between 22nd-century-mean α_s (T_s) and 20th-century-mean α_s (T_s). Values of α_s were weighted by April incoming insolation prior to averaging. Though these values of $\Delta\alpha_s/\Delta T_s$ are based on transient climate change experiments, they agree closely with the values of $\Delta\alpha_s/\Delta T_s$ that would result from equilibrium climate change experiments with the same models because in climate simulations the NH snow pack adjusts in a thermodynamic sense almost instantaneously to anthropogenic forcing [Hall, 2004]. The experiment names corresponding to the numbers on the x-axis are given in table 1.

Figure 4. Scatterplot of the simulated springtime $\Delta\alpha_s/\Delta T_s$ values in the context of climate change (ordinate) vs. the simulated springtime $\Delta\alpha_s/\Delta T_s$ values in the context of the seasonal cycle (abscissa). The numbers of the 17 transient climate change experiments listed in table 1 are used as plotting symbols. The climate change $\Delta\alpha_s/\Delta T_s$ values are simply the data in fig 3b. The seasonal cycle $\Delta\alpha_s/\Delta T_s$ values, based on 20th century climatological means, are calculated by dividing the difference between April and May α_s averaged over NH continents poleward of 30°N by the difference between April and May T_s averaged over the same area. A least-squares fit regression line for the simulations is also shown. The two $\Delta\alpha_s/\Delta T_s$ parameters are highly correlated, with a correlation coefficient of 0.92. The observed springtime $\Delta\alpha_s/\Delta T_s$ value based on the ISCCP data and the ERA40 reanalysis (see text) is plotted as a dashed vertical line, with the grey vertical bar giving an estimate of the statistical error [Neter et al., 1996] in this value. If statistical error only is taken into account, there is a 5% probability that the actual observed value lies outside this grey bar, given the length of the observed time series of $\Delta\alpha_s/\Delta T_s$ and its variance.

Table 1. The names of the models used for transient climate change experiments included in the AR4 assessment. All data for this article were taken from the '720 ppm stabilization experiment', where historical 20th century forcing was imposed on all models, followed by the SRES A1B emission scenario for the 21st century. At year 2100, concentrations of greenhouse gases and other anthropogenic forcing agents were held fixed for the remainder of the experiments, which terminate at year 2200. Though this forcing scenario was imposed on 23 models for the AR4 assessment, only these 17 had a complete time series at the time of this article's composition. For more information about these experiments and the models included in the IPCC AR4 assessment, see http://www-pcmdi.llnl.gov/ipcc/about_ipcc.php.

number	name of model
1	mri_cgcm2_3_2a
2	cnrm_cm3
3	giss_model_e_r
4	iap_fgoals1_0_g
5	cccma_cgcm3_1
6	csiro_mk3_0
7	ncar_pcm1
8	ukmo_hadcm3
9	mpi_echam5
10	ukmo_hadgem1
11	miroc3_2_medres
12	ncar_ccsm3_0
13	miub_echo_g
14	ipsl_cm4
15	gfdl_cm2_0
16	gfdl_cm2_1
17	inmcm3_0

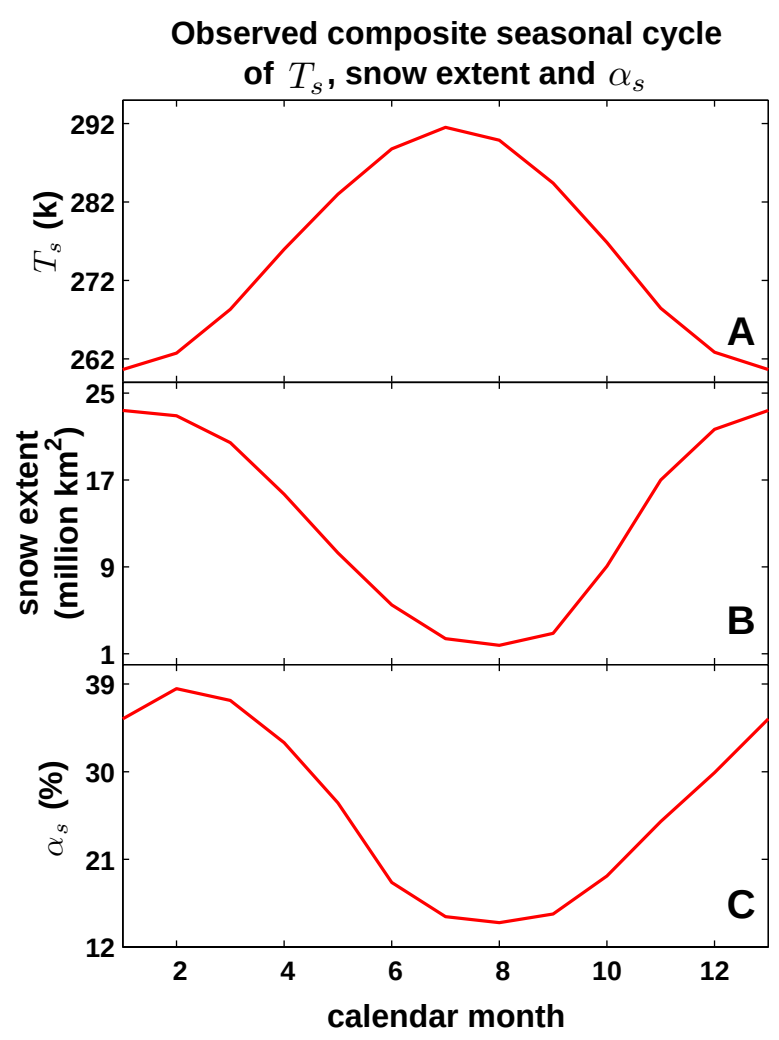
Observed composite seasonal cycle of T_s, snow extent and α_s
T_s (k)
292
282
272
262
A
snow extent (million km^2)
25
17
9
1
B
α_s (%)
39
30
21
12
C
2
4
6
8
10
12
calendar month

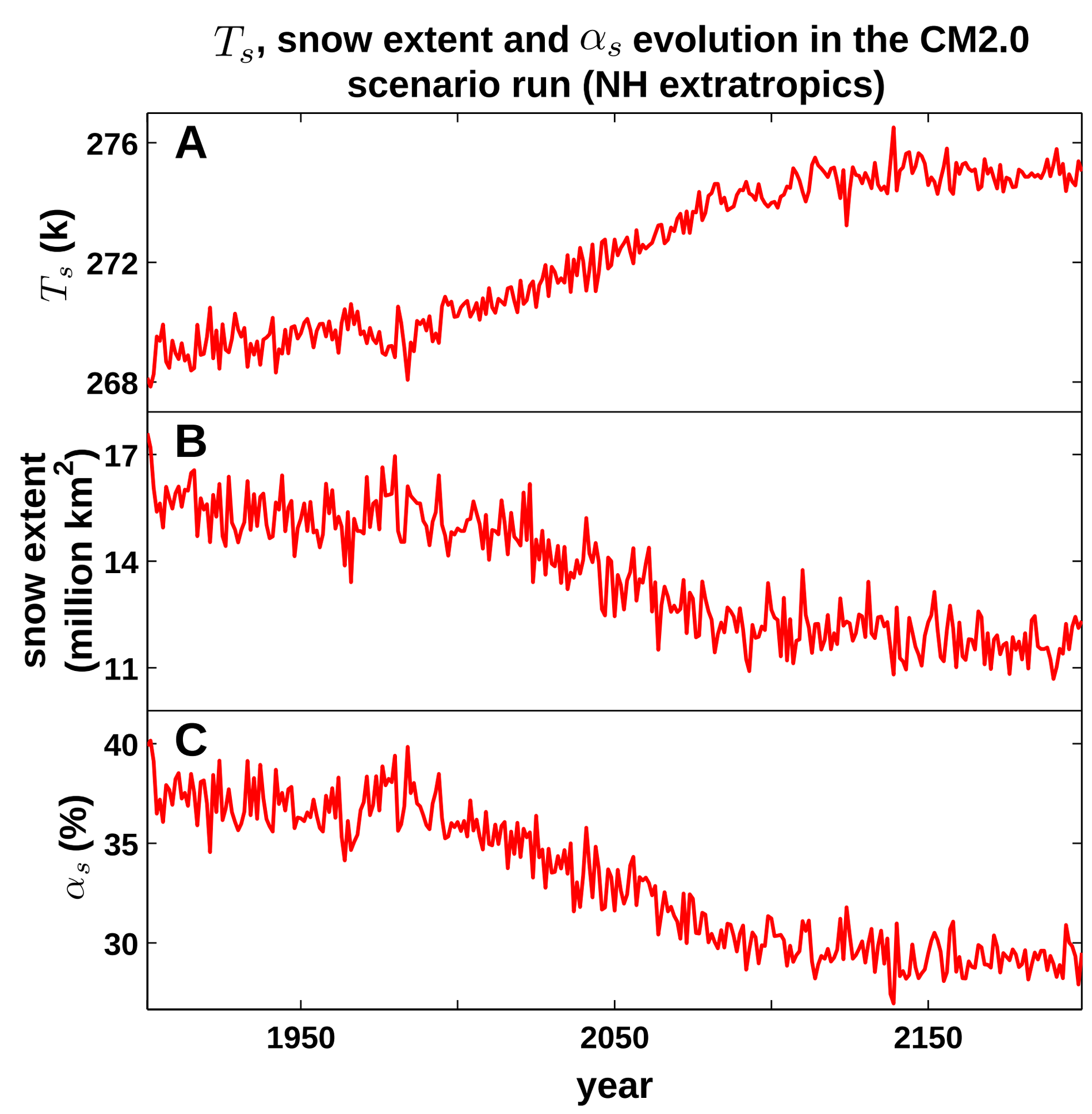
T_s, snow extent and α_s evolution in the CM2.0 scenario run (NH extratropics)
A
B
C
T_s (k)
276
272
268
snow extent (million km^2)
17
14
11
α_s (%)
40
35
30
1950
2050
2150
year

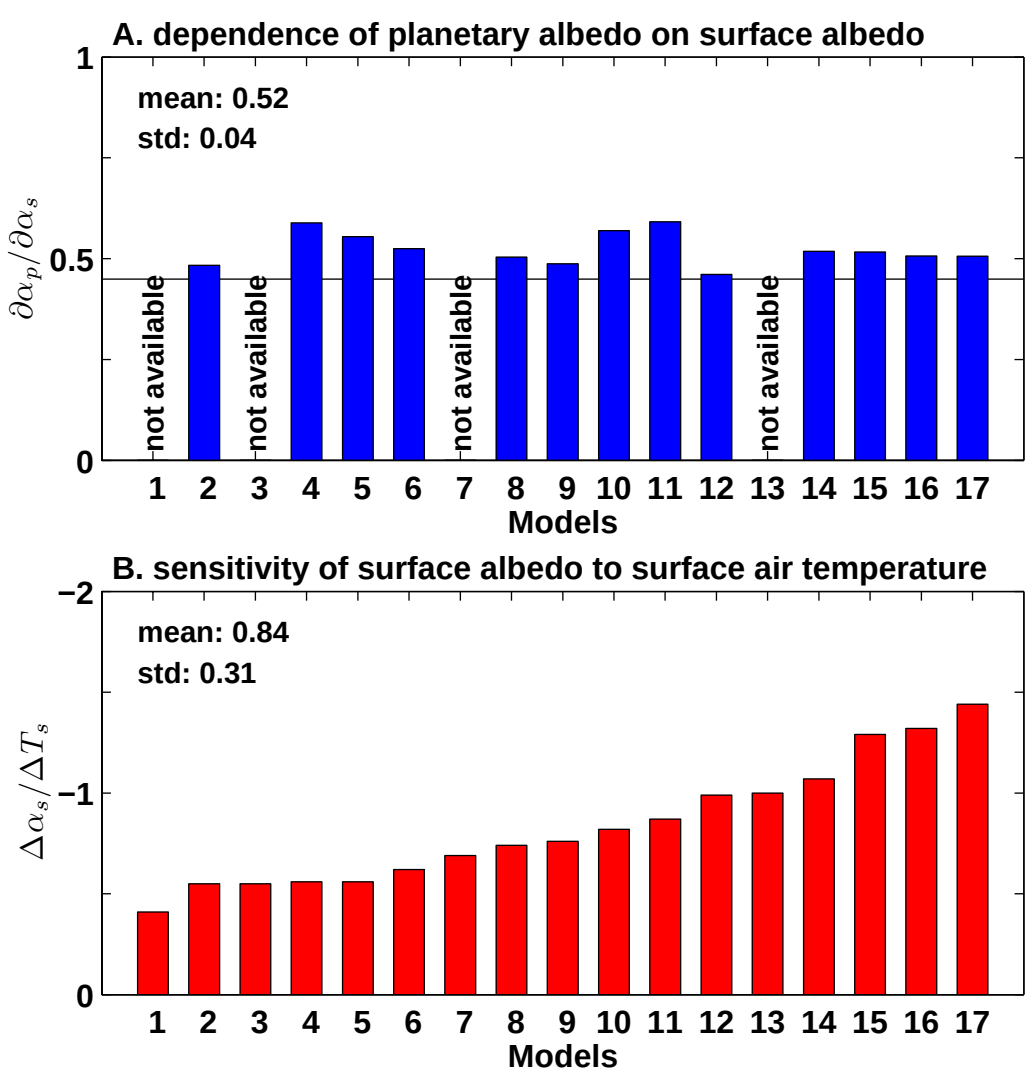
A. dependence of planetary albedo on surface albedo
mean: 0.52
std: 0.04
not available
not available
not available
not available
$\partial\alpha_p/\partial\alpha_s$
1
0.5
0
1 2 3 4 5 6 7 8 9 10 11 12 13 14 15 16 17
Models
B. sensitivity of surface albedo to surface air temperature
mean: 0.84
std: 0.31
$\Delta\alpha_s/\Delta T_s$
−2
−1
0
1 2 3 4 5 6 7 8 9 10 11 12 13 14 15 16 17
Models

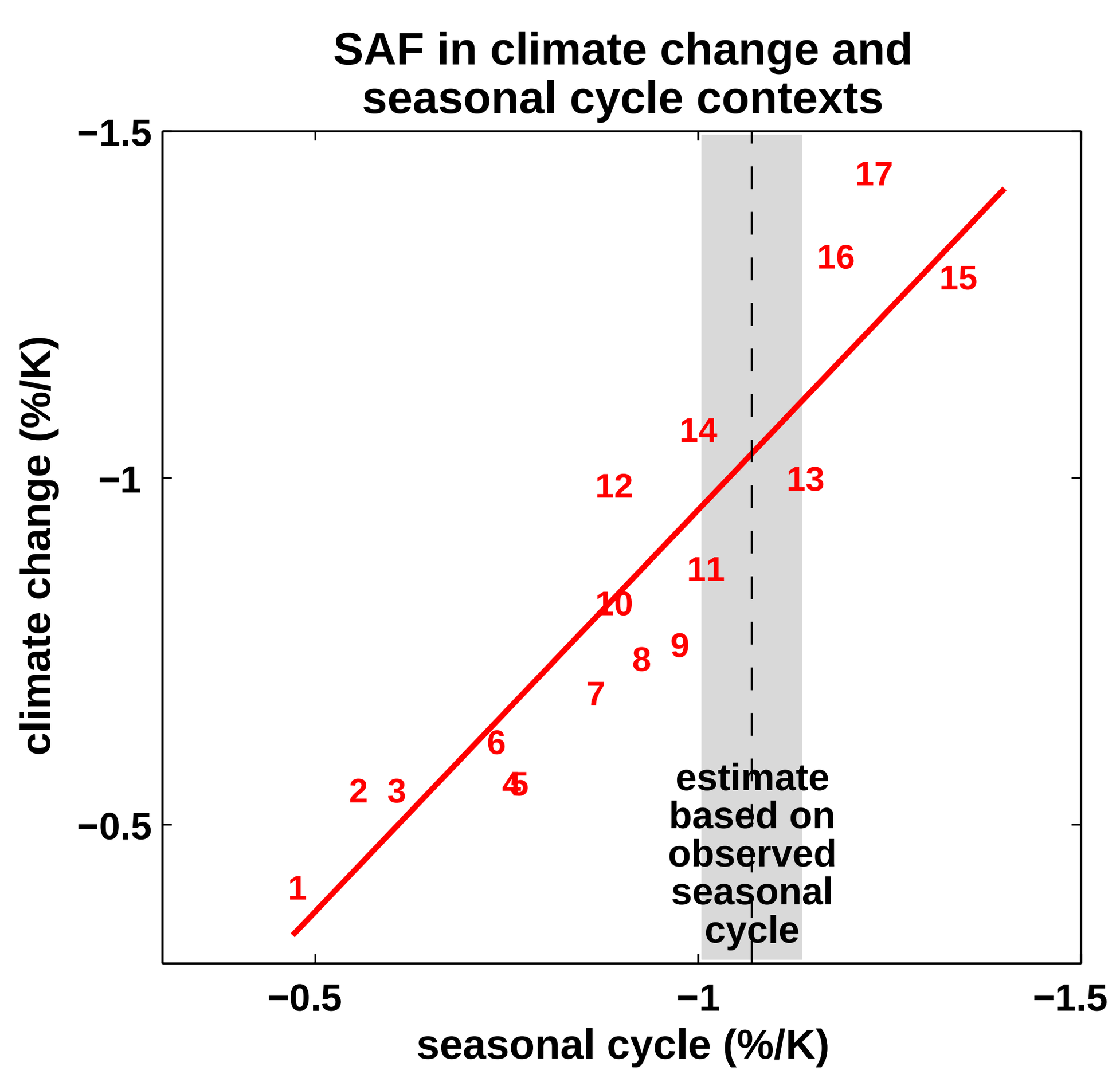
SAF in climate change and seasonal cycle contexts
−1.5
−1
−0.5
climate change (%/K)
−0.5
−1
−1.5
seasonal cycle (%/K)
1
2
3
4
5
6
7
8
9
10
11
12
13
14
15
16
17
estimate based on observed seasonal cycle